Electronic Supplementary Material (ESI) for ChemComm.

Supporting Information

Lanthanide Complex for Secondary Metal Encapsulations and Anion Exchanges with Versatile Colorimetric and Thermochromic Responses

Yan-Qiong Sun, Fang Wan, Xin-Xiong Li, Jian Lin, Tao Wu, Shou-Tian Zheng, and Xianhui Bu

This PDF file includes: **Page**

Section S1 Synthesis and Methods

Synthesis of 1

1,1'-bis((3-carboxylatobenzyl)-4,4'-bipyridinium)dichloride (0.0497 g, 1 mmol) was completely dissolved in a mixed solution of water/ethanol (4 ml: 4 ml) under stirring. The pH of the mixed solution was adjusted to ca. 6.0 by adding 0.5 M aqueous NaOH dropwise. And then, 2 ml of $Eu(NO_3)_3 \cdot 6H_2O$ (0.0150 g, 0.33 mmol) solution was added to the above solution. After the mixture was further stirred for 10 min, the residue was filtered. Yellow crystals (0.0375g, 67.7 % yield based on $Eu(NO_3)_3 \cdot 6H_2O$) were obtained after the filtrate was allowed to stand for 2 days.

Synthesis of 2Cd

As-synthesized yellow crystals **1** (75 mg, ca. 0.04 mmol) were dissolved and refluxed in a 10 ml 0.04 M $Cd(NO_3)_2$ solution for 12 hours. After cooling to room temperature, the solution was allowed to stand for one day to form new yellow crystals **2Cd**.

Release of Cd^{2+} ions from 2Cd

The sample **2Cd** (10 mg) was soaked in 2 ml water for 5 days. About 8 mg sample was recovered by filtering and used for EDS and PXRD measurements.

Syntheses of 2M (**M** = Zn^{2+}, Cu^{2+}, Ni^{2+}, Co^{2+}, Ba^{2+}, Ca^{2+}, and Mg^{2+})

For each M^{2+} ion, as-synthesized crystals **1** (75 mg, ca. 0.04 mmol) were dissolved and refluxed in 10 ml 0.04 M $M(NO_3)_2$ solutions for 12 hours. After cooling to room temperature, the solution was allowed to stand for one day to form new crystals **2M**.

Syntheses of 2Mn

As-synthesized crystals **1** (75 mg, ca. 0.04 mmol) were dissolved and refluxed in 10 ml 0.04 M $MnCl_2$ solution for 12 hours. After cooling to room temperature, the solution was allowed to stand for one day to form new yellow crystals **2Mn**.

Anion-Exchange Experiments

Anion-exchange experiments were performed by immersing 50 mg sample **1** in 2 mL ethanol solvents of 2 mmol different anions including SCN^-, N_3^-, NO_2^-, SO_4^{2-}, N_3^-, Cl^-, Br^-, and I^- for 12 h to give different anion-exchanged products.

Solvent accessible volumes of 1 and 2Cd.

An analysis using the PLATON software tool (PLATON VOIDS probe diameter 1.2 Å: A. L. Spek, *J. Appl. Crystallogr,* 2003, **36**, 7) indicates that the extra-framework volumes for **1** and **2Cd** are 33.9% and 21.2% of the total unit cell volumes, respectively.

Single-crystal X-ray diffraction: Crystals **1**, **3**, and **4** were collected on a Bruker APEX II CCD area diffractometer equipped with a fine focus, 2.0 kW sealed tube X-ray source (MoKα radiation, λ = 0.71073 Å̊) operating at 293(2) K. The empirical absorption correction was based on equivalent reflections. Structures were solved by direct methods followed by successive difference Fourier methods. Computations were performed using SHELXTL and final full-matrix refinements were against F^2. The contribution of disordered solvent molecules to the overall intensity data of structure **1** was treated using the SQUEEZE method in PLATON. Crystal **2Cd** was collected on a SuperNova diffractometer with graphite monochromated Cu-Kα radiation (λ = 1.54184 Å) at 293(2) K. The empirical absorption correction was based on equivalent reflections. Structures were solved by direct methods followed by successive difference Fourier methods. Computations were performed using SHELXTL and final full-matrix refinements were against F^2. The contribution of disordered solvent molecules to the overall intensity data of structures **1** and **2Cd** were treated using the SQUEEZE method in PLATON. CCDC-1476371-1476374 contains the supplementary crystallographic data for **1**, **2Cd**, **3**, and **4**, respectively. These data can be obtained free of charge from The Cambridge Crystallographic Data Centre via www.ccdc.cam.ac. uk/data_request/cif.

Others: Powder X-ray diffraction patterns were obtained by using a PANalytical X'Pert PRO X-ray powder diffractometer operating at 40 kV and 40 mA with Co Kα radiation (λ = 1.78901 Å). The data collection was performed with a step size of 5^o and counting time of 60s per step. The 2θ angular range is from 5 to 45 ^{o}. UV–vis diffuse reflectance spectral measurements were carried out using a Perkin–Elmer Lambda 900 spectrometer. The spectrophotometer was calibrated against the surface of $BaSO_4$ for 100% reflectance over the wavelength range under consideration. Energy-dispersive spectrometry (EDS) elemental analyses on single crystals were performed with a NOVA NANOSEM230 EDAX scanning electron microscope (SEM) equipped with energy dispersive spectroscopy (EDS) detector. Inductively coupled plasma (ICP) analyses were performed on a HORIBA JobinYvonUltima2 inductively coupled plasma. Luminescent spectra were recorded on an Edinburgh Instruments FLS980 TCSPC spectrofluorimeter equipped with both continuous-wave (450 W) and pulse xenon lamps.

Section S2 Additional Tables

Table S1. ICP analyses of **2Cd** and **2M** (**M** = Zn^{2+}, Cu^{2+}, Ni^{2+}, Co^{2+}, Mn^{2+}, Ba^{2+}, Ca^{2+}, and Mg^{2+}).

Compounds	Experimental values from ICP		
	M (wt%)	Eu (wt%)	Mole Ratio of M/Eu
2Cd	4.55	6.37	0.97 (Cd/Eu)
2Zn	1.87	8.64	0.50 (Zn/Eu)
2Cu	2.41	7.41	0.98 (Cu/Eu)
2Ni	1.13	9.00	0.33 (Ni/Eu)
2Co	1.21	8.78	0.36 (Co/Eu)
2Mn	1.79	8.39	0.59 (Mn/Eu)
2Ba	1.27	9.52	0.15 (Ba/Eu)
2Ca	0.78	9.26	0.32 (Ca/Eu)
2Mg	0.33	9.44	0.22 (Mg/Eu)

Table S2. Semiquantitative EDS analysis of **2Cd**. The data is shown in the following table in which the total amount of Cd and Eu is normalized to 100%.

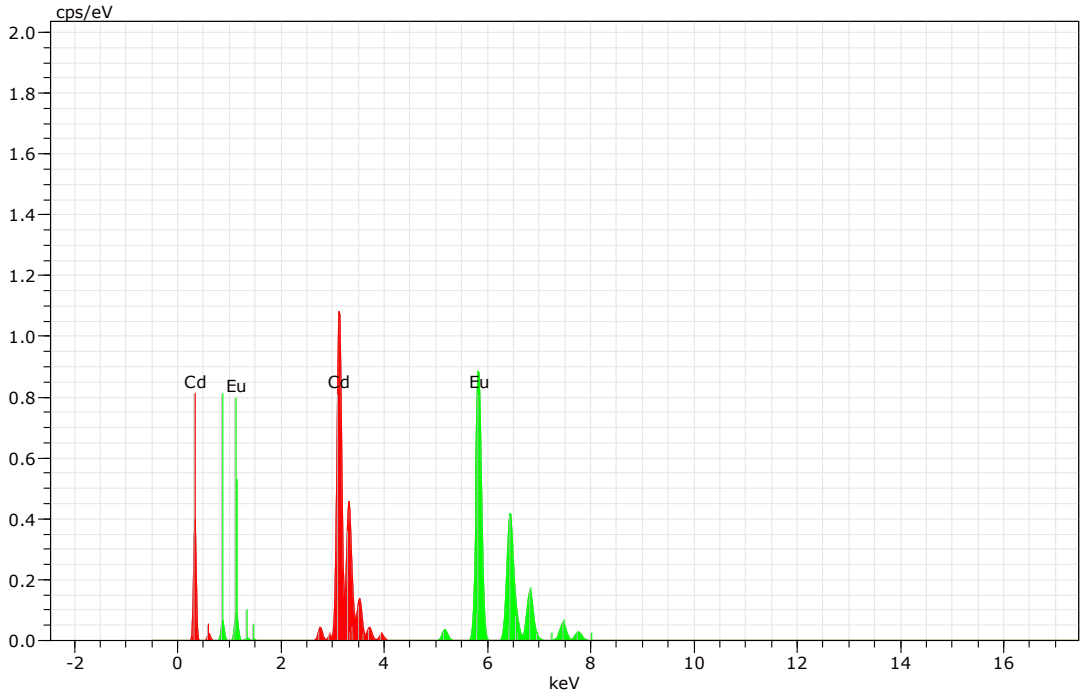

Experimental values from EDS			Calculated values from formula
Cd (wt%)	Eu (wt%)	Mole Ratio of Cd/Eu	Mole Ratio of Cd/Eu
40.74	59.26	0.90	1.0

Table S3. EDS analysis of soaked crystal **2Cd**. The total amount of Cd and Eu is normalized to 100%.

Experimental values from EDS	Soak time in deionized water

Cd (wt%)	Eu (wt%)	Mole Ratio of Cd/Eu	
26.62	73.38	0.49	1 hour
6.51	93.49	0.10	5 days

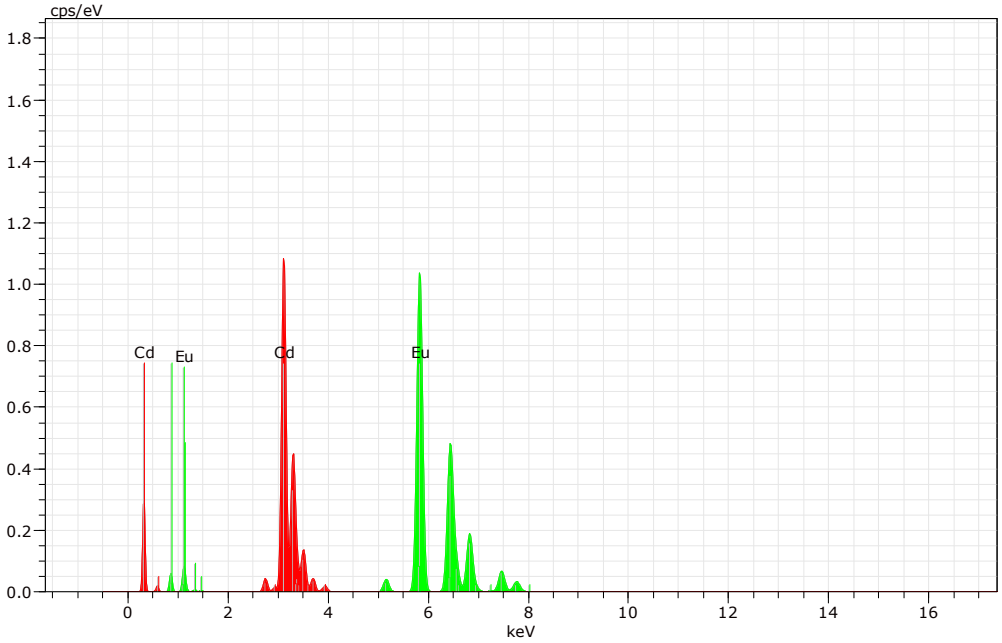

After soaking sample **2Cd** in deionized water for 1 hour

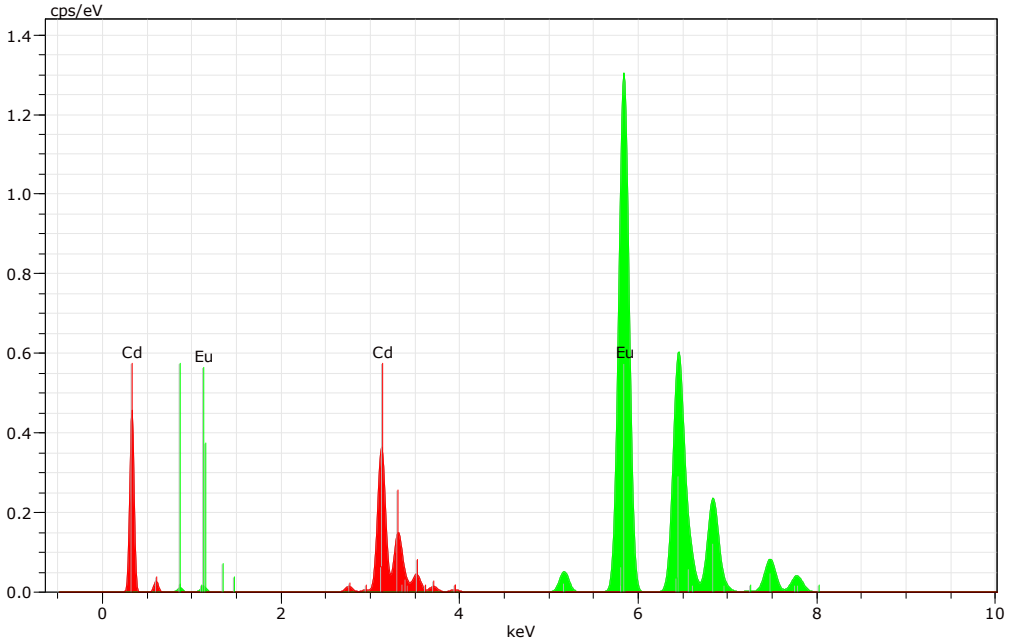

After soaking sample **2Cd** in deionized water for 5 days

Table S4. Crystallographic data for **1**, **2Cd**, **3**, and **4**.

Compound	**1**	**2Cd**

Empirical formula	$C_{78}H_{66}EuN_9O_{24}$	$C_{78}H_{66}CdEuN_{11}O_{35}$
Formula weight	1665.36	1981.77
Crystal system	Cubic	Cubic
Space group	$P2_13$	$P2_13$
a/Å	20.898(3)	20.5090(1)
V/Å^3	9126(2)	8626.5(1)
Z	4	4
D_c/g cm^{-3}	1.122	1.526
μ/mm^{-1}	0.748	7.934
F(000)	3160	4008
θ range (deg)	$1.38 \leq \theta \leq 22.93$	$3.05 \leq \theta \leq 66.58$
Reflections collected	19794	17022
unique data (R_{int})	4222 (0.0531)	4237 (0.0681)
Limiting indices	$-12 \leq h \leq 22$	$-22 \leq h \leq 14$
	$-14 \leq k \leq 17$	$-24 \leq k \leq 21$
	$-22 \leq l \leq 22$	$-24 \leq l \leq 24$
Completeness	99.9 %	98.9 %
Data/restraints/parameters	4222 / 0 / 303	4237 / 0 / 370
Goodness-of-fit on F^2	1.041	1.054
R_1[a], wR_2[b] [$I>2\sigma(I)$]	0.0559, 0.1544	0.0714, 0.1993
R indices (all data)	0.0643, 0.1595	0.0737, 0.2034
Absolute structure parameter	0.04(2)	0.07(1)
$\Delta\rho_{max}$, $\Delta\rho_{min}$ (e.Å^{-3})	0.780, -0.299	0.977, -0.705
Compound	**3**	**4**
Empirical formula	$C_{26}H_{22}Cl_4Hg_2N_2O_5$	$C_{52}H_{48}N_8O_{25}Pb_2$

Formula weight	985.44	1599.36
Crystal system	Monoclinic	Monoclinic
Space group	*C*2/*c*	*P*2(1)/*c*
a/Å	20.2500(3)	16.7770(3)
b/Å	12.1502(17)	12.3446(19)
c/Å	13.9840(4)	13.270(2)
β/°	123.951(2)	96.886(2)
V/Å^3	2854.0(9)	2728.5(7)
Z	4	2
D_c/g cm^{-3}	2.293	1.947
μ/mm^{-1}	11.160	6.260
F(000)	1840	1560
θ range (deg)	$2.07 \le \theta \le 25.14$	$2.05 \le \theta \le 25.05$
Reflections collected	5921	10871
unique data (R_{int})	2534 (0.0223)	4771 (0.0239)
Limiting indices	$-24 \le h \le 23$	-19<=h<=17
	$-14 \le k \le 11$	-14<=k<=14
	$-14 \le l \le 16$	-14<=l<=15
Completeness	99.2 %	98.8 %
Data/restraints/parameters	2534 / 0 / 177	4771 / 0 / 398
Goodness-of-fit on F^2	1.132	1.181
R_1[a], wR_2[b] [$I>2\sigma(I)$]	0.0331, 0.0999	0.0323, 0.1002
R indices (all data)	0.0419, 0.1152	0.0415, 0.1174
$\Delta\rho_{max}$, $\Delta\rho_{min}$ (e.Å^{-3})	1.151, -1.496	1.264, -1.072

[a] $R_1 = \sum||F_o| - |F_c||/\sum|F_o|$; [b] $wR_2 = \{\sum[w(F_o^2 - F_c^2)^2/\sum[w(F_o^2)^2]]^{1/2}$.

Section S3 Additional Structural Figures

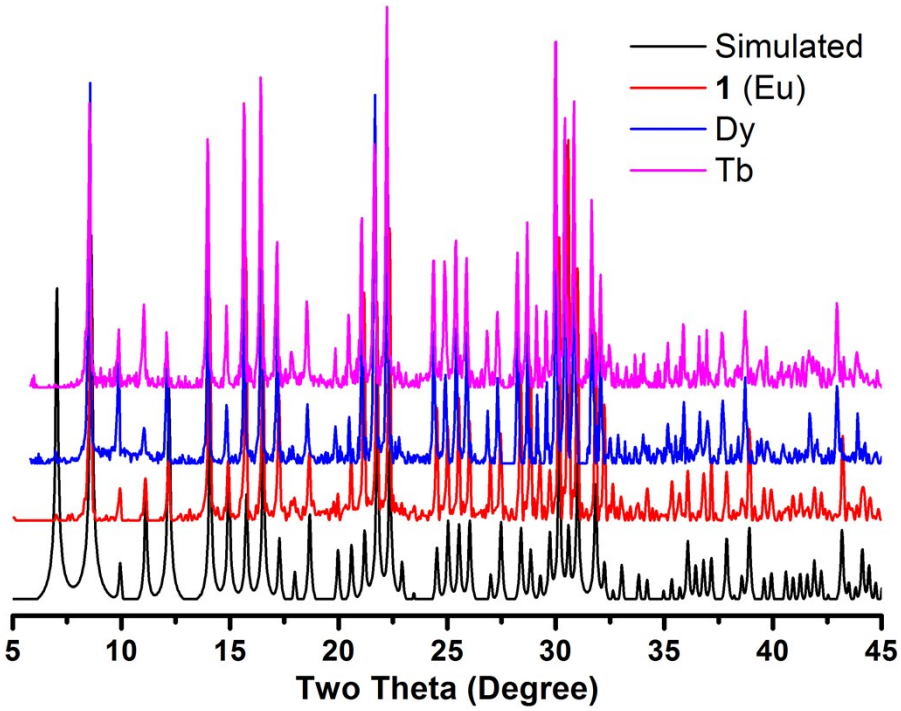

Figure S1. PXRD patterns of simulated **1**, as-synthesized sample **1**, $Dy(bcbpy)_3(H_2O)_3 \cdot 3NO_3$, and $Tb(bcbpy)_3(H_2O)_3 \cdot 3NO_3$, showing the as-synthesized sample **1** is pure phase and compounds $Dy(bcbpy)_3(H_2O)_3 \cdot 3NO_3$ and $Tb(bcbpy)_3(H_2O)_3 \cdot 3NO_3$ are isostructural with **1**.

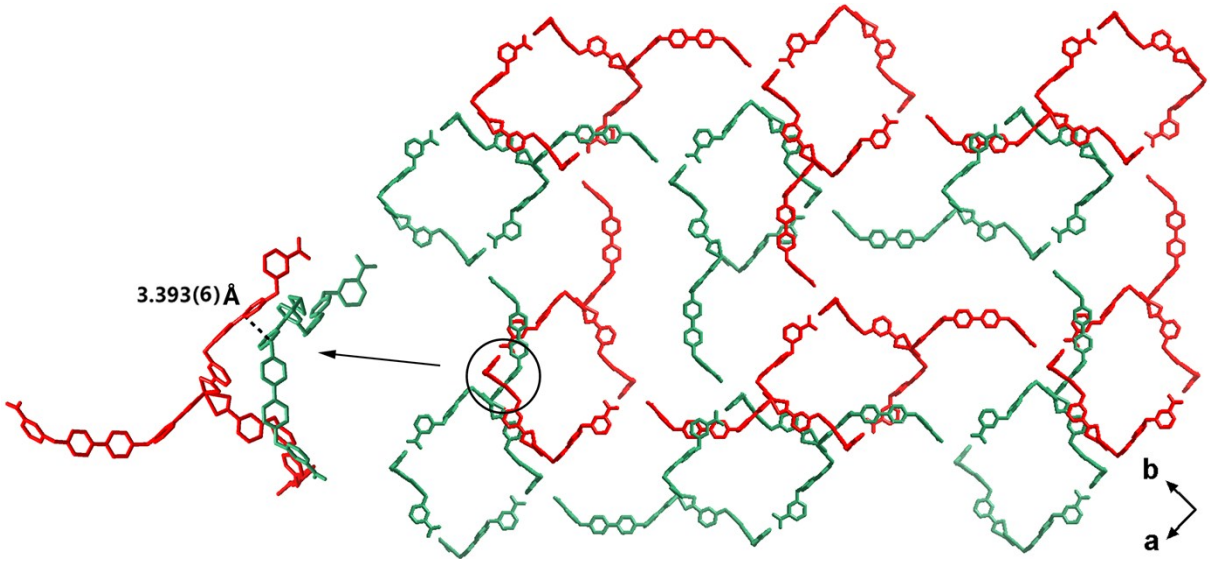

Figure S2. View of packing mode between two adjacent supramolecular grids, showing the inter-grid aromatic π-π interactions within structure **1**.

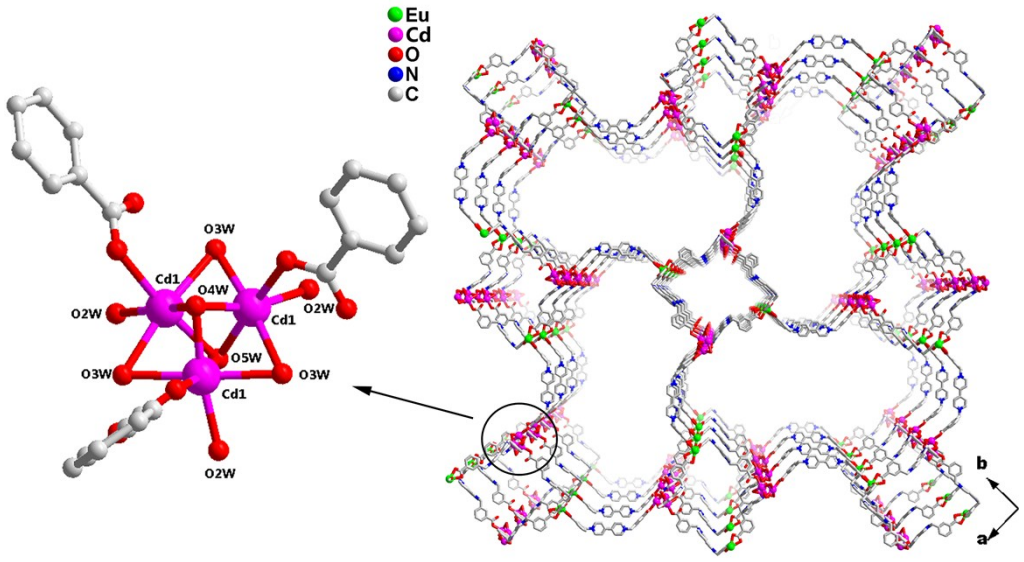

Figure S3. View of disordered model of the encapsulated Cd^{2+} ion in **2Cd**. Each Cd^{2+} ion is disordered over three sites to form a trimer-like cluster with C_3 symmetry. The occupancy of disordered Cd is freely refined to 0.3120, showing the occupancy of each cadmium position can be fixed to 1/3. Within the trimer, each Cd^{2+} ion is 6-coordinated with one carboxylic oxygen atom from one bcbpy (Cd-O: 2.329(8) Å) and five water molecules (Cd-H_2O: 2.073(12) - 2.297(11) Å) to form an octahedral configuration. The occupancy of Cd^{2+} ion is also confirmed by ICP analysis. Similar to Cd^{2+} ion, water molecules O2W and O3W are also disordered over three sites with refined occupancy of 1/3 for each position. While, different from O2W and O3W, both water molecules O4W and O5W with occupancy of 1/3 are ordered because they locate at special positions (on the *C*3 rotation axis).

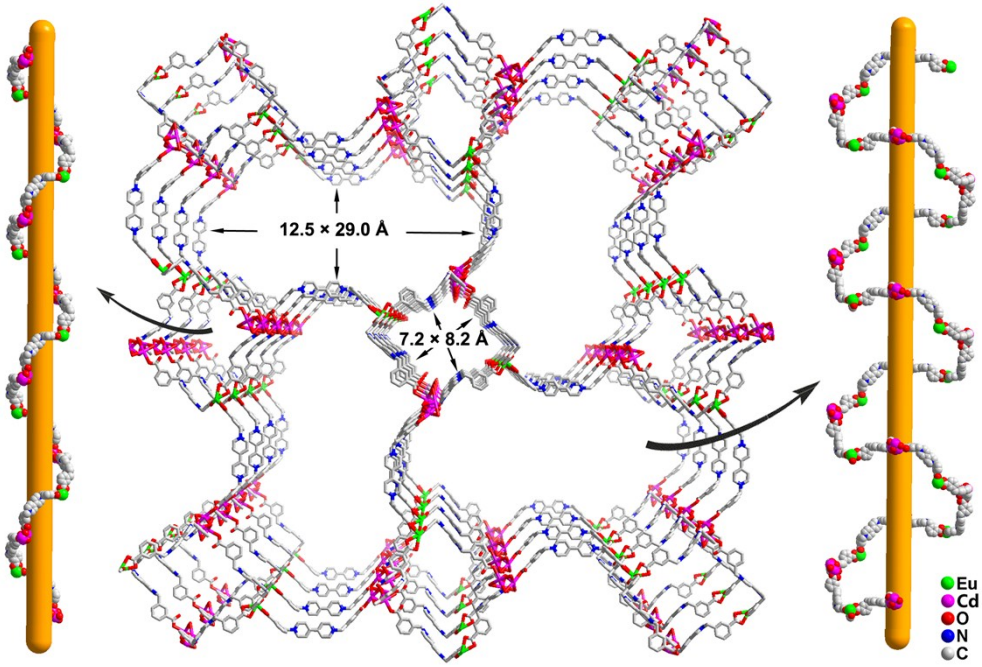

Figure S4. View of a single pseudo heterometallic network in **2Cd**, showing helical square channels and ellipse channels running along the *c*-axis direction.

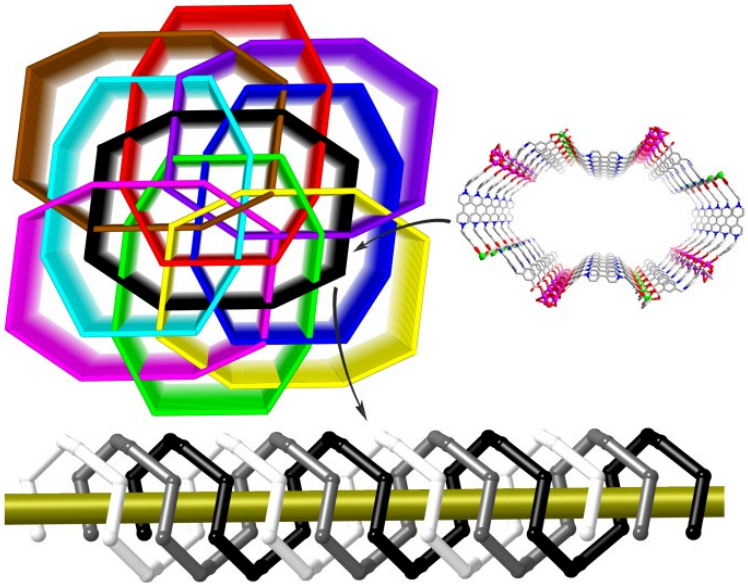

Figure S5. Diagram illustrating a pseudo 27-fold interpenetrating structure of **2Cd**.

The highly porous nature of a single pseudo heterometallic network leads to a 27-fold interpenetration in the overall structure **2Cd**. The 27-fold interpenetration can be illustrated by its local structural segment of the helical ellipse channels (Figure S5). Viewed along the *c*-axis, there are 9 sets of interpenetrating helical ellipse channels as shown by 9 different colors. Meanwhile, each set of helical ellipse channel contains 3 sets of coaxial helical chains (same handedness) intertwined with each other in a mutually parallel mode, giving rise to a total of 27-fold (9×3) structure **2Cd**. Notably, though interpenetration is a common phenomenon in porous MOFs, the degree of interpenetrations in known MOFs is usually ≤ 10. Especially, high-fold (> 18) interpenetrating MOFs are very rare (H. Wu, J. Yang, Z. M. Su, S. R. Batten, J. F. Ma, *J. Am. Chem. Soc*, **2011**, *133*, 11406-11409).

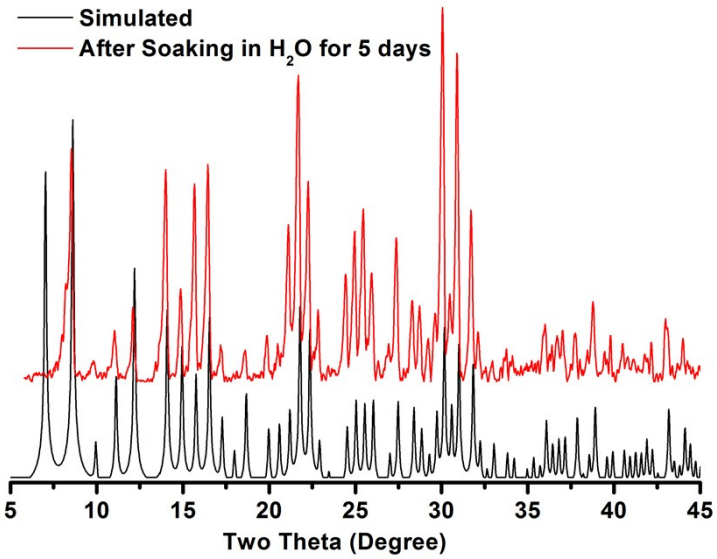

Figure S6. PXRD patterns of **2Cd**.

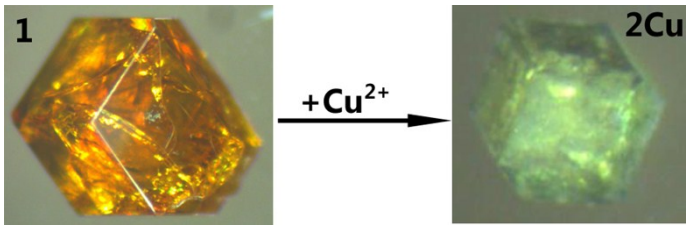

Figure S7. View of crystals **1** and **2Cu**, showing a clear crystal color difference between them.

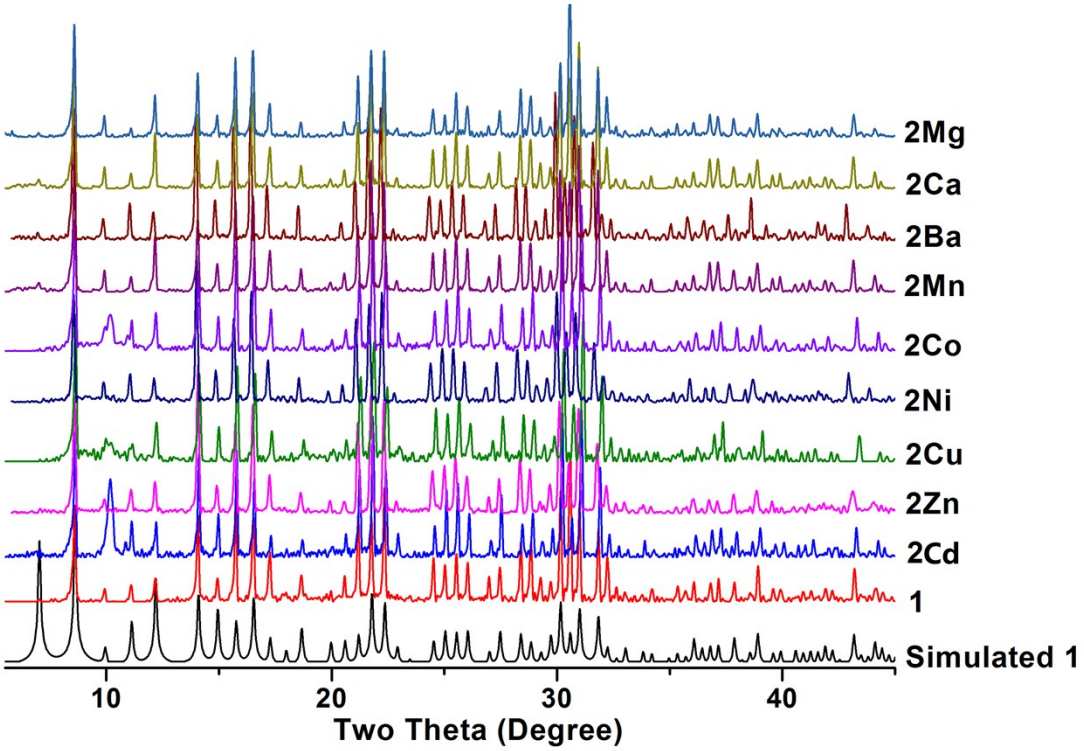

Figure S8. PXRD patterns of simulated compound **1** and as-synthesized samples **1**, **2Cd**, and **2M**.

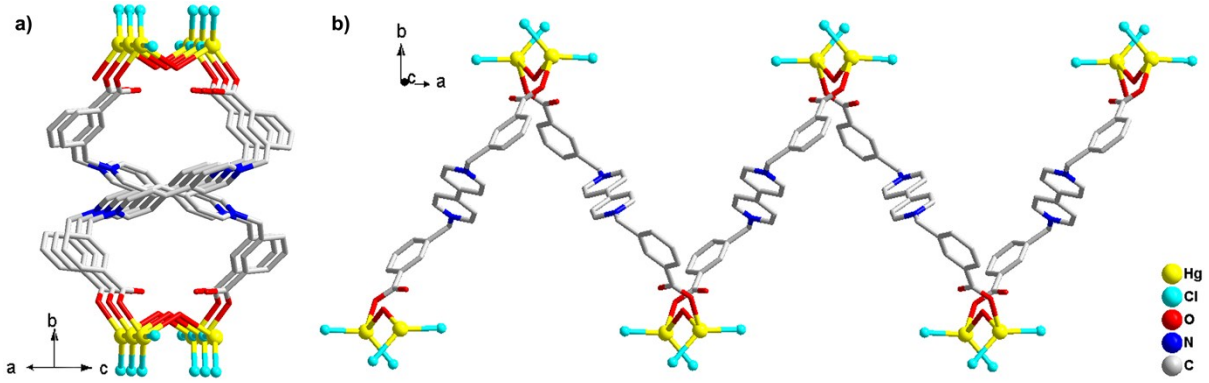

Figure S9. (a) and (b) View of 1D chain $Hg_2Cl_4(bcbpy)(H_2O)$ along [101] and [001] directions, respectively.

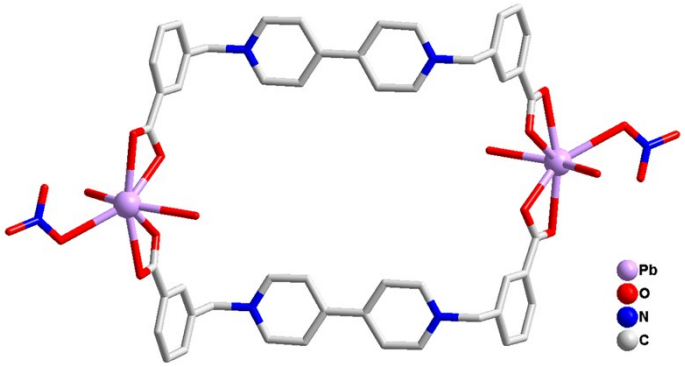

Figure S10. View of 0D binuclear lead complex $[Pb_2(bcbpy)_2(H_2O)_6(NO_3)_2]^{2+}$.

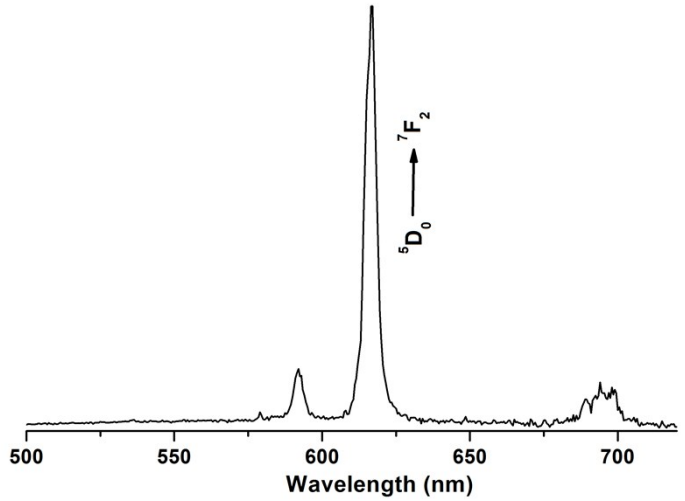

Figure S11. Emission spectrum of **1** (excited at 395 nm).

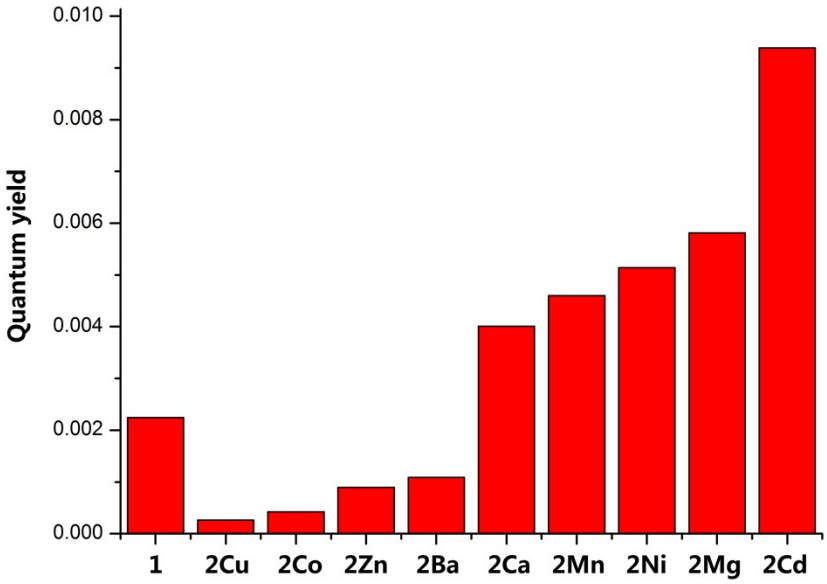

Figure S12. The fluorescence quantum yields of emission peak at 617 nm of **1**, **2Cd**, and **2M**, showing the encapsulation of Cd^{2+} ion can remarkably increase the Eu^{3+} luminescence intensity.

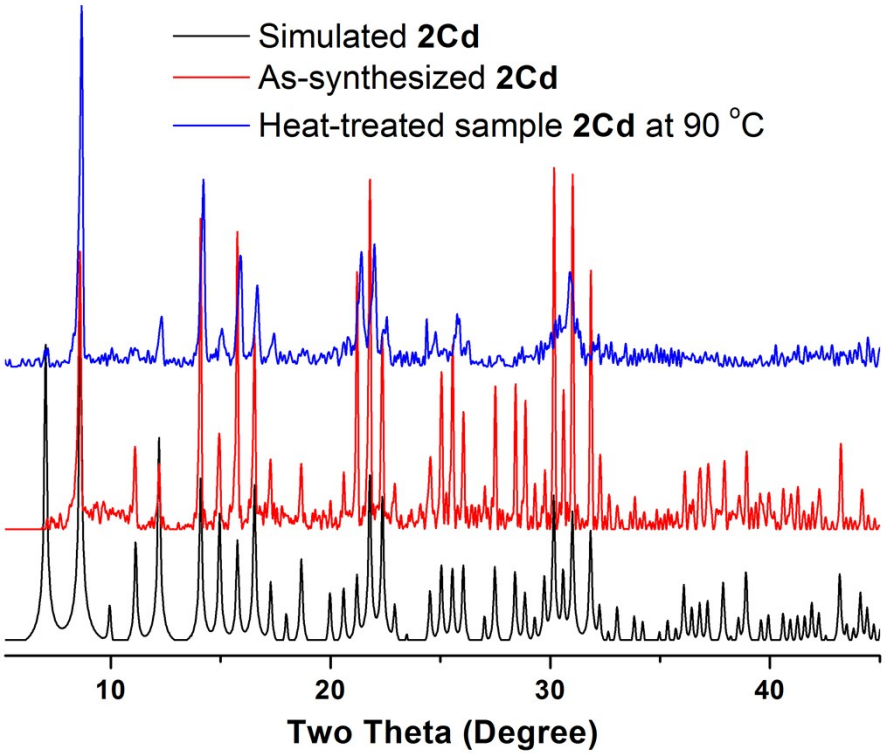

Figure S13. PXRD patterns of **2Cd**, showing **2Cd** keeps its crystalline from RT to 90 °C.

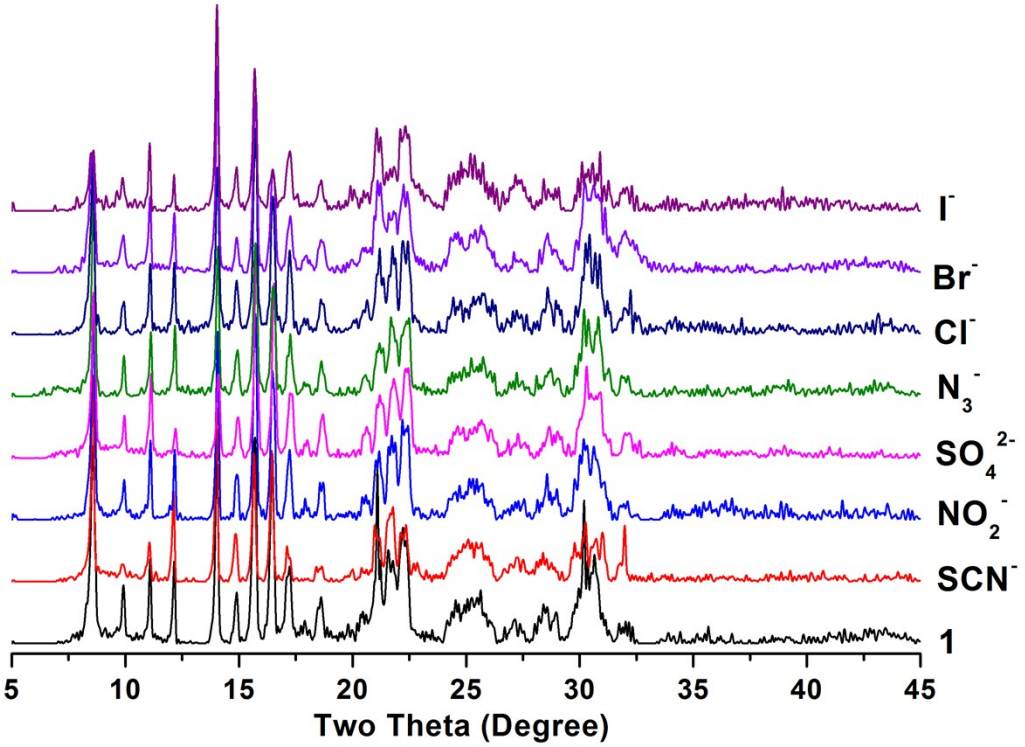

Figure S14. PXRD patterns of **1** and its anion-exchanged samples, showing structure **1** remained intact throughout all anion-exchange processes.

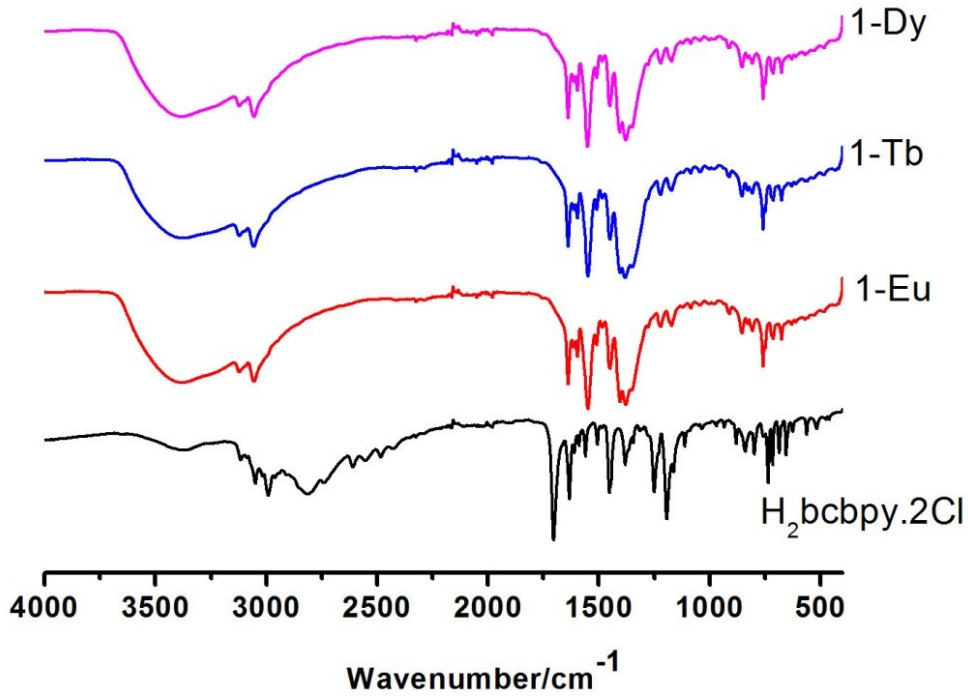

Figure S15. IR spectra of **1-Eu**, **1-Dy**, **1-Tb,** and H_2bcpy.2Cl ligand.

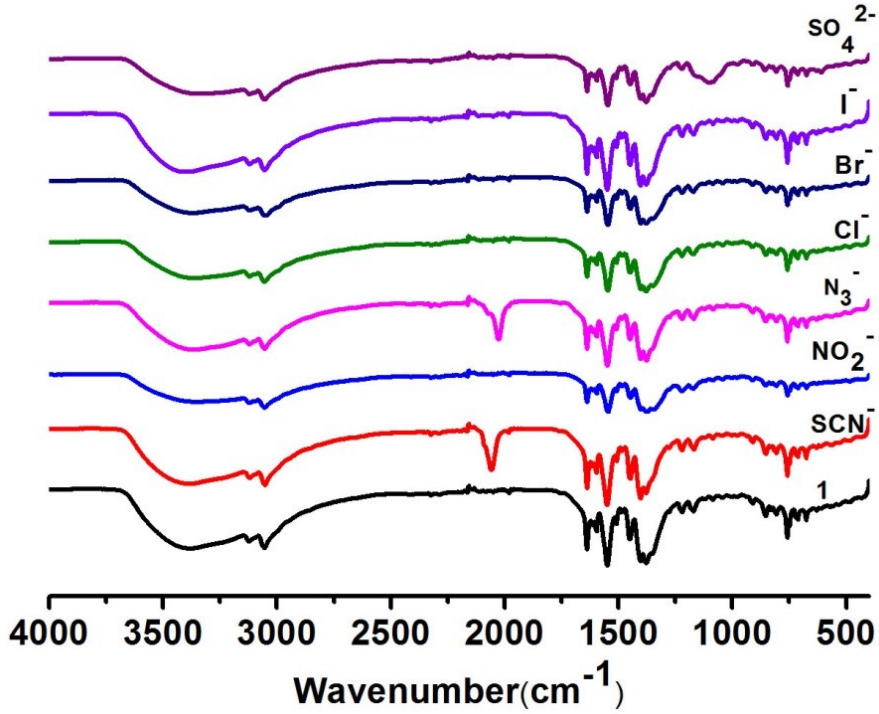

Figure S16. IR spectra of **1** and ion-exchanged samples.

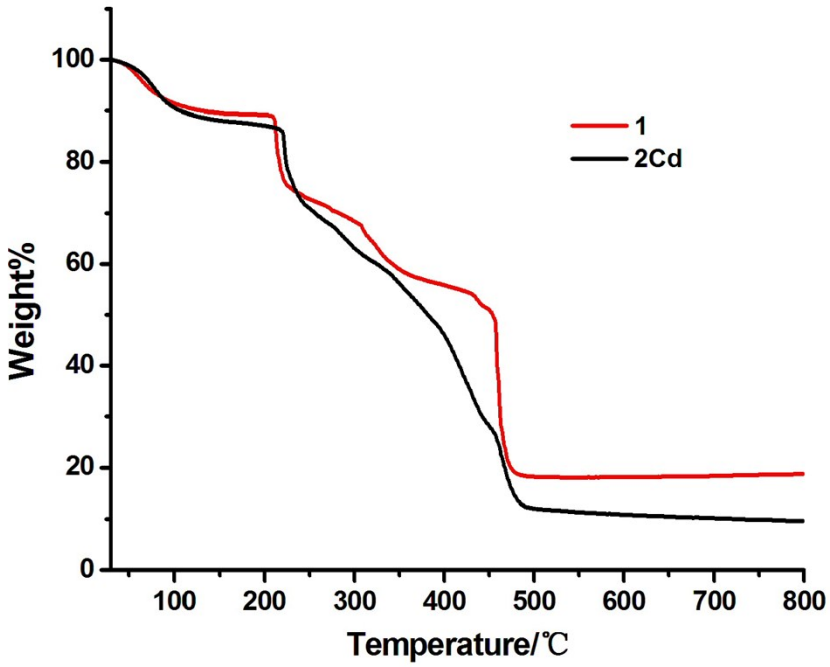

Figure S17. TG curves of **1-Eu** and **2Cd.**

The thermogravimetric analyses were carried out in flowing air with a heating rate of 10 ˚C min^{-1} in the temperature range from 30 ˚C to 800 ˚C for the compounds **1** and **2Cd** (Figure S17). Both TGA curves show two major weight loss stages, which are fallen in the regions 34 ˚C – 100 ˚C and 220 ˚C – 480 ˚C, respectively. The first weight loss processes of **1** and **2Cd** are attributed to the loss of solvent guests, while the second loss processes correspond to the collapse of structures of **1** and **2Cd**. The TG curves show **1** and **2Cd** maintain their structures up to about 200 ˚C.

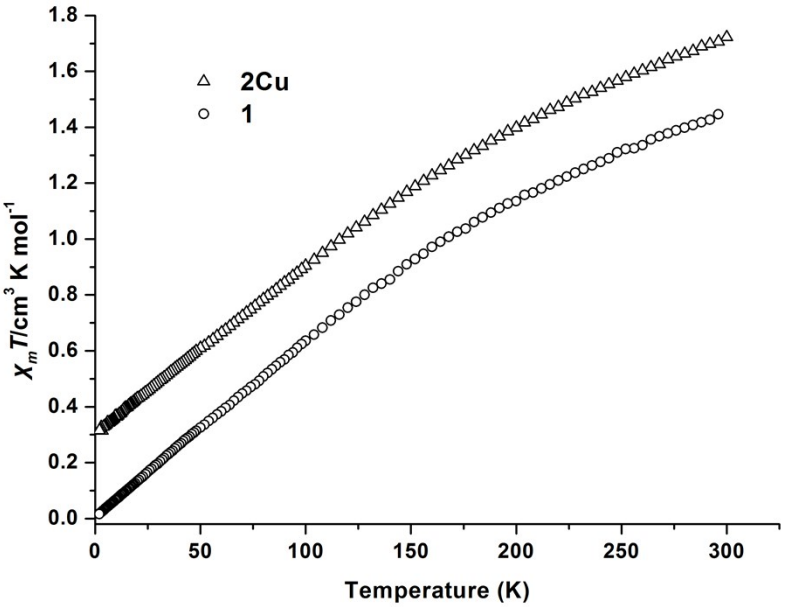

Figure S18. Temperature dependence of $\chi_m T$ values for **1** and **2Cu**.

The magnetic susceptibilities of **1** and **2Cu** were measured in 2-300 K and are shown in Figure S18. At room temperature, the observed $\chi_m T$ value of **1** is 1.45 $cm^3mol^{-1}K$, slightly less than the value 1.5 $cm^3 \cdot mol^{-1} \cdot K$ for a Eu^{3+} ion calculated by Van Vleck equation allowing for population of the excited state with higher values of *J* at 293 K (*Inorg. Chem*, 2005, **44**, 862; *Cryst. Growth Des*. 2014, **14**, 5495). Upon cooling, $\chi_m T$ decreases continuously as a result of the depopulation of the levels with nonzero *J* values. At the lowest temperature, $\chi_m T$ is close to zero, indicating a $J = 0$ ground state of the Eu^{3+} ion ($^7F_0$). The experimental $\chi_m T$ value of **2Cu** at room temperature is 1.80 $cm^3 \cdot mol^{-1} \cdot K$ per formula, which is expected for a Eu^{3+} ion (1.5 $cm^3 \cdot mol^{-1} \cdot K$) and a Cu^{2+} ion (0.375 $cm^3 \cdot mol^{-1} \cdot K$). Upon cooling, the $\chi_m T$ values of **2Cu** decrease to a minimum of 0.32 $cm^3 \cdot mol^{-1} \cdot K$ at 2 K.

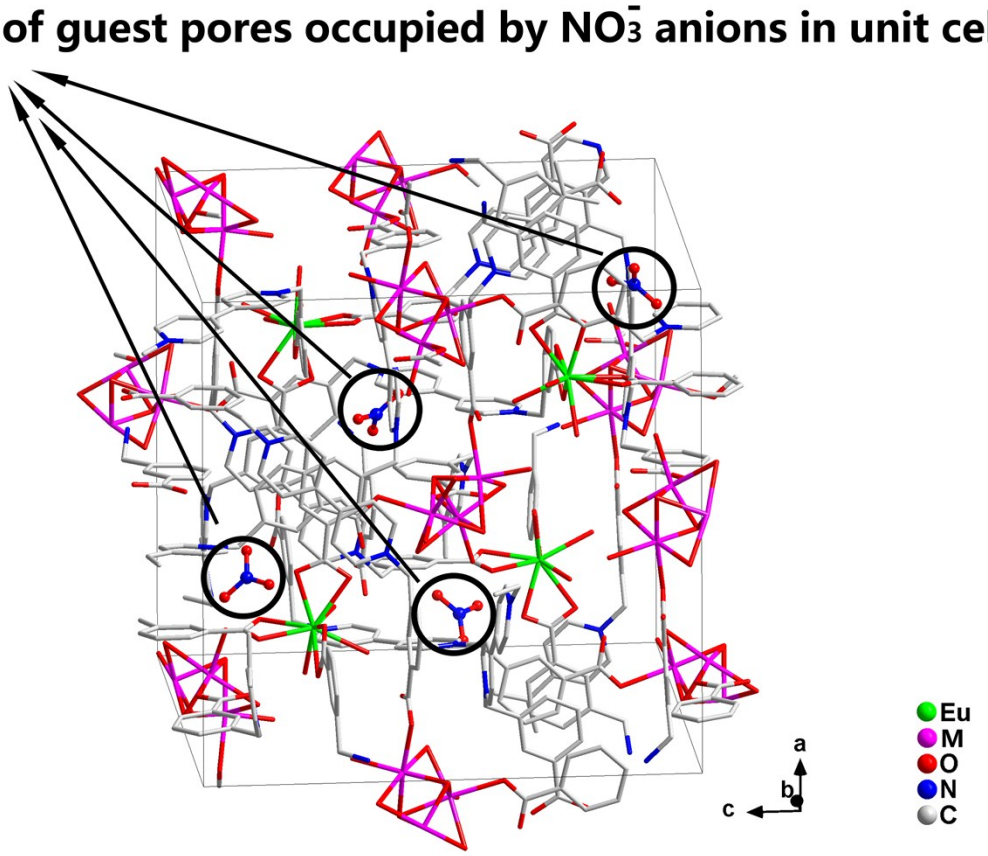

Figure S19. View of different pores in the unit cell of **1** respectively occupied by the encapsulated of M^{2+} cations and isolated NO_3^- anions.

There are two kinds of completely different pores within the structure of **1**. As described in manuscript (Page 2, Para 2 and 3), the first is the voids defined by the uncoordinated carboxylate groups of bcbpy ligands (as shown in figure 1), which is responsible for the encapsulation of metal cations. The second is extra-framework pores (can be viewed as guest pores) occupied by isolated NO_3^- anions. Once the NO_3^- anions are ion-exchanged with other anions, other anions will occupy the extra-framework pores. These extra-framework pores distribute inside the complicated 3D supramolecular packing structure of **1**, as shown in figure S19.